

Nonlinear electrostatic ion cyclotron wave collapse and formation of wave packets in the presence of trapped electrons

Akash Biswas¹,* Debkumar Chakraborty¹, and Samiran Ghosh¹

Department of Applied Mathematics, University of Calcutta, 92 Acharya Prafulla Chandra Road, Kolkata-700009, India

 (Received 18 July 2022; revised 12 September 2022; accepted 20 October 2022; published 8 November 2022)

The weakly nonlinear and dispersive electrostatic ion cyclotron wave dynamics in the presence of Schamel distributed trapped electrons is studied in collisionless plasmas. The dynamics of the nonlinear wave is shown to be governed by a Schamel-Ostrovsky type equation. Analytical and numerical solutions of this equation reveal the collapse of a solitary (localized) pulse at a critical time that depends on the trapping parameter and the strength of the magnetic field. The time-dependent computational result is noteworthy, which predicts the formation of wave packets (wave group) beyond the critical time. The results are in good agreement with the astrophysical observations in auroral plasmas.

DOI: [10.1103/PhysRevE.106.055206](https://doi.org/10.1103/PhysRevE.106.055206)

I. INTRODUCTION

The study of nonlinear wave propagation in a magnetized plasma is an interesting topic of research from both experimental and theoretical points of view as the inclusion of magnetic field in plasmas can change the entire wave dynamics by introducing a different space and timescales compared to unmagnetized plasma [1]. In a magnetized electron-ion plasma, one of the low-frequency eigenmodes is the electrostatic ion cyclotron wave (EICW) mode [2], which is observed in laboratory plasmas [3,4].

Moreover, several satellite (S3-3, ISEE-1, Viking, Polar, GEOTAIL, and FAST) observations also confirm the existence of EICWs in the auroral magnetosphere at altitudes between $(3-8) \times 10^3$ km and beyond [5–13]. These waves are believed to be responsible for the plasma heating [14].

The astrophysical [5–13], theoretical [15–23], and experimental [24–26] observations reveal that the EICWs exhibit nonlinear coherent (spiky, sawtooth, bipolar) structures in response to the large amplitude disturbances. These coherent structures are believed to be associated with the multiharmonic EICWs due to the ion shear flow in the absence of trapped electrons [22,23,26].

However, in the auroral acceleration region, a significant fraction of the electrons are trapped by the EICWs between the ion cavities [27]. Also, the FAST satellite observation [11] and simulation [28] on auroral magnetosphere confirm the existence of electron holes; the signature of the presence of trapped electrons. In the presence of a strong magnetic field, the electron holes are generated through the process of magnetic reconnection [29–32]. These holes are characterized by a localized positive potential well in which a population of electrons is trapped [33,34] and

are well explained by the Schamel's distribution (a vortex distribution) [35–38]. The transport properties of nonlinear EICWs in the presence of trapped electrons are not well investigated [39].

In this article, we present a theoretical and computational study on the weakly nonlinear and dispersive transport properties of EICWs in the presence of trapped electrons in collisionless and homogeneous plasmas. The trapped electrons are incorporated in the plasma through the Schamel's distribution [35–38]. The external uniform and static magnetic field is assumed to be weak under the assumption that the ion cyclotron frequency $\Omega_i (= eB_0/m_i)$, e is the magnitude of the electric charge, B_0 is the magnitude of the magnetic field, and m_i is the ion mass) is small compared to the ion oscillation frequency $\omega_{pi} (= \sqrt{n_0 e^2 / (\epsilon_0 m_i)})$, n_0 is the equilibrium plasma density, and ϵ_0 is the permittivity) so that the ratio $\Omega = \Omega_i / \omega_{pi} \sim O(\sqrt{\epsilon})$ (where ϵ is a measure of the smallness of the perturbed amplitude). It is shown that the weakly nonlinear dynamics of EICW is governed by a rotation modified Schamel equation or Schamel-Ostrovsky equation (SOE) due to the Lorentz force induced rotation. This derived nonlinear SOE is solved analytically with the help of a two-time-scale Krylov-Bogoliubov-Mitropolsky (KBM) perturbation method [40] and numerically for the typical auroral plasma parameters. Depending on the strength of the magnetic field and trapping parameter, both the analytical and the computational results predict (i) the existence of a critical time τ_{cr} (that determines the life of a solitary pulse) at which the nonlinear wave collapses, the formation of (ii) oscillatory tails and (iii) EICW packets (wave group) in the long time. The computational results are in qualitative agreement with the astrophysical observations [12].

The article is organized in the following manner: The physical model with basic equations and the derivation of the SOE are provided in Sec. II. The approximated analytical solution of the SOE is derived in Sec. III. The computational results with graphical representations are discussed in Sec. IV. Finally, the results and their possible applications in the context of auroral plasmas are briefly discussed in Sec. V.

*Corresponding author: akash1995.biswas@gmail.com;

Present address: Department of Mathematics, Katwa College, Katwa, Purba Bardhaman-713130, India.

II. BASIC EQUATIONS AND DERIVATION OF SCHAMEL-OSTROVSKY EQUATION

We consider a fully ionized, unbounded and homogeneous plasma consisting of cold ions and trapped electrons immersed in a static uniform magnetic field $\vec{B} = B_0 \hat{z}$. Further, without any loss of generality it is assumed that the perturbations are in the x - z plane [1,15–17,39]. The low-frequency EICWs are ion waves propagating almost but not exactly perpendicular to \vec{B} . Here, the ions move essentially in a plane perpendicular to \vec{B} so that the electric field $\vec{E} \approx -\hat{x}\partial_x\varphi$ [$\varphi(x, z)$ is the electrostatic potential] and the wave vector $\vec{k} \approx k_x \hat{x}$ ($k_z \sim 0$), whereas the much lighter electrons can move along \vec{B} to establish charge neutrality [1]. Actually, the small deviation from the 90° relative to \vec{B} allows for a component of the wave electric field parallel to \vec{B} which causes the electrons to distribute along the field lines (here in the \hat{z} direction) at any instant behaving like massless fluid and its perpendicular motion becomes unimportant [1,15–17,39].

Also for the EICWs in the auroral region, both the electrons and the ions satisfy the relation

$$\frac{\Omega_i}{\omega_{pi}} \ll 1 \ll \frac{\Omega_e}{\omega_{pe}} \Rightarrow \rho_e \ll \lambda_D \ll \rho_{si}, \quad (1)$$

where $\Omega_e (= eB_0/m_e)$, m_e is the electron mass) and $\omega_{pe} [= \sqrt{n_0 e^2 / (\epsilon_0 m_e)}]$ are the electron cyclotron and plasma frequencies. Also $\lambda_D [= \sqrt{\epsilon_0 T_{ef} / (n_0 e^2)}]$, T_{ef} is the free electron temperature] is the plasma Debye length, $\rho_e [= V_{Te} / \Omega_e]$, $V_{Te} = (T_{ef} / m_e)^{1/2}$ the electron thermal velocity] is the electron gyroradius and $\rho_{si} (= c_s / \Omega_i)$, $c_s = \sqrt{T_{ef} / m_i}$ is the ion acoustic speed) is the ion acoustic gyroradius. The relation (1) suggests the kinetic and fluid descriptions of the electrons and ions, respectively, to study the EICWs. Accordingly, we consider the collisionless normalized Vlasov equation for electrons in the \hat{z} direction (as electrons are distributed along \hat{z}), which in the ion timescale (stationary) can be read [35] as

$$v_{ez} \frac{\partial f_e}{\partial z} + \delta^{-1} \frac{\partial \phi}{\partial z} \frac{\partial f_e}{\partial v_{ez}} = 0, \quad \phi = \frac{e\varphi}{T_{ef}}, \quad \delta = \frac{m_e}{m_i}. \quad (2)$$

Here f_e and v_{ez} are the normalized electron distribution and velocity (along the z axis; normalized by c_s), respectively. The space scale is normalized by λ_D . The general solution of Eq. (2) is of the form $f_e \equiv f_e(\vec{v}_e, \phi)$. The most commonly used solution is the Maxwell-Boltzmann distribution which follows equilibrium thermodynamics. The nonlinear EICWs are well studied in the presence of equilibrium electron distribution [1,15–17].

However, to model the trapped electron distribution in the presence of an external uniform magnetic field, first we estimate the contribution of the cross-field electron drifts in the distribution. Thus, we consider the total energy (normalized) of the electrons as

$$\mathcal{E}_{\text{tot}} = \phi + \frac{\delta}{2} (v_{e\perp}^2 + v_{ez}^2). \quad (3)$$

Taking $v_{e\perp}$ as the $\vec{E} \times \vec{B}$ drift, one can estimate [39]

$$\frac{\delta}{2} v_{e\perp}^2 = \frac{1}{2} \left(\frac{\omega_{pe}}{\Omega_e} \right)^2 (\nabla \phi \times \hat{z})^2 < \frac{1}{2} \left(\frac{\omega_{pe}}{\Omega_e} \right)^2 (\nabla \phi)^2. \quad (4)$$

It has already been established [39] that for Schamel distributed trapped electrons $(\nabla \phi)^2 \sim O(\phi^{5/2})$ and $\omega_{pe} / \Omega_e \ll 1$ [relation (1)], which indicate that the $v_{e\perp}^2$ term in \mathcal{E}_{tot} as well as in the corresponding trapping condition is negligible and f_e is then effectively one-dimensional parallel to \vec{B} [39]. Thus the trapping occurs here in the \hat{z} direction. Accordingly, f_e is considered as the Schamel's nonequilibrium distribution [35], i.e., $f_e = f_{ef} + f_{et}$ [$f_{ef(t)}$ is the free (trapped) electron distribution function] where

$$f_{ef} = \sqrt{\frac{\delta}{2\pi}} \exp \left[-\frac{\delta}{2} \left(v_{ez}^2 - \frac{2\phi}{\delta} \right) \right], \quad |v_{ez}| > \sqrt{2\phi/\delta},$$

$$f_{et} = \sqrt{\frac{\delta}{2\pi}} \exp \left[-\frac{\delta\beta}{2} \left(v_{ez}^2 - \frac{2\phi}{\delta} \right) \right], \quad |v_{ez}| \leq \sqrt{2\phi/\delta}. \quad (5)$$

Here $\beta = T_{ef} / T_{et}$ is the trapping parameter and T_{et} is the trapped electron temperature. The electron distribution [Eq. (5)] represents Maxwellian, flattop, and trapped (a vortexlike excavated trapped electron distribution that corresponds to the electron hole in phase space) for $\beta = 1$, $\beta = 0$, and $\beta < 0$, respectively [35]. Finally, taking the first moment of the distribution [Eq. (5)], in the small amplitude limit ($\phi \ll 1$), the electron density can be expressed [35–38] as

$$n_e = 1 + \phi - \frac{4b}{3} \phi^{3/2} + \frac{1}{2} \phi^2 + \dots, \quad b = \frac{(1-\beta)}{\sqrt{\pi}}. \quad (6)$$

The $\beta < 0$ region where b is relatively large is of interest in our present investigation.

The normalized ion fluid equations [1,15,16] are

$$\frac{\partial n}{\partial t} + \frac{\partial}{\partial x} (nu) = 0, \quad (7)$$

$$\frac{\partial u}{\partial t} + u \frac{\partial u}{\partial x} = -\frac{\partial \phi}{\partial x} + \Omega v, \quad (8)$$

$$\frac{\partial v}{\partial t} + u \frac{\partial v}{\partial x} = -\Omega u. \quad (9)$$

Here the timescale (t) is normalized by ω_{pi}^{-1} . The ion fluid velocities u (along the x axis) and v (along the y axis) are normalized by c_s . The ion density n is normalized by equilibrium density (n_0). Finally, for the closure, we consider the Poisson's equation

$$\frac{\partial^2 \phi}{\partial x^2} = n_e - n. \quad (10)$$

Linearizing these equations [Eqs. (6)–(10)] in a homogeneous background, we derive the dispersion relation of the EICW [1] as

$$\tilde{\omega}^2 = \frac{\tilde{k}^2}{1 + \tilde{k}^2} + \Omega^2 \Rightarrow \omega^2 = \frac{k_x^2 c_s^2}{1 + k_x^2 \lambda_D^2} + \Omega_i^2, \quad (11)$$

where $\tilde{\omega} (= \omega / \omega_{pi})$ and $\tilde{k} (= k_x \lambda_D)$ are normalized frequency and the wave number, respectively.

To study the weakly nonlinear dynamics of EICWs in the presence of a relatively large number of trapped electrons ($b > 1$), we introduce the stretched variables [37]

$$\xi = \sqrt[4]{\epsilon} (x - Vt), \quad \tau = \sqrt[4]{\epsilon^3} t, \quad (12)$$

where V is the normalized phase velocity of the linear wave. The dynamical variables are expanded as

$$\begin{aligned} n &= 1 + \epsilon n^{(1)} + \epsilon^{3/2} n^{(2)} + \dots, \\ u &= \epsilon u^{(1)} + \epsilon^{3/2} u^{(2)} + \dots, \\ v &= \epsilon^{5/4} v^{(1)} + \epsilon^{7/4} v^{(2)} + \dots, \\ \phi &= \epsilon \phi^{(1)} + \epsilon^{3/2} \phi^{(2)} + \dots. \end{aligned} \quad (13)$$

In the auroral region, plasma density $n_0 \sim 10^7 m^{-3}$, $B_0 \sim 1.2 \times 10^{-5} T$ and the predominant ions are H^+ ($m_i \sim 1.6 \times 10^{-27}$ kg) [6,20,21]. These estimate $\omega_{pi} \sim 4 \times 10^3$ s $^{-1}$ and $\Omega_i \sim 1.2 \times 10^3$ s $^{-1}$ so that $\Omega \sim 0.3$. Thus to incorporate the effects of this low Ω , we consider the following consistent scaling:

$$\Omega \sim O(\sqrt{\epsilon}). \quad (14)$$

Substituting Eqs. (12)–(14) in the set of basic Eqs. (7)–(10) and then equating the coefficients of different powers of ϵ , we obtain the first- and second-order relations among the dynamical variables. The first-order relations are

$$V \frac{\partial n^{(1)}}{\partial \xi} = \frac{\partial u^{(1)}}{\partial \xi}, \quad V \frac{\partial u^{(1)}}{\partial \xi} = \frac{\partial \phi^{(1)}}{\partial \xi}, \quad (15)$$

$$n^{(1)} = \phi^{(1)}, \quad V \frac{\partial v^{(1)}}{\partial \xi} = \Omega u^{(1)}. \quad (16)$$

These relations self-consistently determine

$$V = 1 \quad \text{and} \quad n^{(1)} = u^{(1)} = \phi^{(1)} = \psi \quad (\text{say}). \quad (17)$$

The second-order relations are

$$-V \frac{\partial n^{(2)}}{\partial \xi} + \frac{\partial n^{(1)}}{\partial \tau} + \frac{\partial u^{(2)}}{\partial \xi} = 0. \quad (18)$$

$$-V \frac{\partial u^{(2)}}{\partial \xi} + \frac{\partial u^{(1)}}{\partial \tau} + \frac{\partial \phi^{(2)}}{\partial \xi} = \Omega v^{(1)}. \quad (19)$$

$$\frac{\partial^2 \phi^{(1)}}{\partial \xi^2} = -n^{(2)} + \phi^{(2)} - b(\phi^{(1)})^{3/2}. \quad (20)$$

Eliminating all the second-order variables and using the first-order relations [Eqs. (16) and (17)], we finally obtain the following nonlinear partial differential equation that describes the weakly nonlinear dynamics of EICWs in the presence of trapped electrons:

$$\frac{\partial}{\partial \xi} \left(\frac{\partial \psi}{\partial \tau} + \frac{3b}{4} \sqrt{\psi} \frac{\partial \psi}{\partial \xi} + \frac{1}{2} \frac{\partial^3 \psi}{\partial \xi^3} \right) = \epsilon \psi, \quad \epsilon = \frac{\Omega^2}{2}. \quad (21)$$

Here the term ϵ appears due to the magnetic field induced Lorentz force. In the absence of magnetic field ($\epsilon = 0$), Eq. (21) reduces to the well-known Schamel equation for nonlinear ion acoustic wave in electron-ion plasmas [35],

$$\frac{\partial \psi}{\partial \tau} + \frac{3b}{4} \sqrt{\psi} \frac{\partial \psi}{\partial \xi} + \frac{1}{2} \frac{\partial^3 \psi}{\partial \xi^3} = 0. \quad (22)$$

Thus the derived equation is a rotation modified Schamel equation. However, the rotation modified Korteweg–de Vries equation is known as the Ostrovsky equation, which describes the nonlinear internal waves in a rotating ocean [41–44]. Thus, we call Eq. (21) a Schamel–Ostrovsky equation. A similar type equation was used to study the nonlinear wave dynamics in elasticity theory for fractional order strain intensity [45].

However, SOE is not derived and studied before in plasma physics.

III. ANALYTICAL SOLUTION

Multiplying Eq. (21) by ψ and integrating over ξ , we get the total energy of the system as

$$\begin{aligned} \frac{\partial \mathcal{E}}{\partial \tau} + \mathcal{E}_{\text{rot}} &= 0, \quad \mathcal{E} = \int_{-\infty}^{\infty} \psi^2 d\xi, \\ \mathcal{E}_{\text{rot}} &= \epsilon \left[\left(\int_{-\infty}^{\infty} \psi d\xi \right)^2 - \int_{-\infty}^{\infty} \left(\psi \int_{-\infty}^{\xi} \psi d\xi \right) d\xi \right]. \end{aligned} \quad (23)$$

Here the first term is the rate of change of wave energy (\mathcal{E}), while the second term (\mathcal{E}_{rot}) is the rate of change of energy due to the Lorentz force induced rotation and thereby the total energy of the plasma system is conserved. However, the SOE [Eq. (21)] is not exactly integrable (solvable) as the wave energy is not conserved. Therefore, here we derive an approximated analytical solution using the KBM perturbation method [40,46,47]. Interestingly, in the absence of magnetic field ($\epsilon = 0$), Eq. (21) reduces to the Schamel equation [Eq. (22)] which possesses the solitary wave solution [35]

$$\psi = N \operatorname{sech}^4 \left[\Delta^{-1} \left(\xi - \frac{2b\sqrt{N}}{5} \tau \right) \right], \quad \Delta = \sqrt{\frac{20}{b\sqrt{N}}}, \quad (24)$$

where N , Δ , and $2b\sqrt{N}/5$ are the amplitude, width, and velocity of the solitary wave.

To study a finite but small effect of ϵ on the solution (24), we assume that the N is a slowly varying function of time (τ), instead of a constant (in the absence of ϵ) and perform a two-timescale [fast (τ_0) and slow (τ_1)] KBM perturbation analysis [40,46,47] of Eq. (21) with

$$\tau_0 = \tau, \quad \tau_1 = \epsilon \tau. \quad (25)$$

Also introduce a new space variable ζ in a frame moving with the solitary wave as

$$\zeta = \Delta^{-1} \left(\xi - \frac{2b}{5} \int_0^\tau \sqrt{N} d\tau \right). \quad (26)$$

In the presence of ϵ , we seek a solution of Eq. (21) of the form

$$\psi(\zeta, \tau, \epsilon) = \psi_0(\zeta, \tau_0, \tau_1) + \epsilon \psi_1(\zeta, \tau_0) + O(\epsilon^2). \quad (27)$$

Substituting (26), (25), and (27) into (21), we have the order unity relation as

$$\frac{\partial \psi_0}{\partial \tau_0} + \mathcal{L}[\psi_0] = 0, \quad \mathcal{L} \equiv \frac{1}{\kappa} \frac{\partial}{\partial \zeta} \left[\frac{\partial^2}{\partial \zeta^2} + \left(30 \sqrt{\frac{\psi_0}{N}} - 16 \right) \right], \quad (28)$$

where $\kappa = 2(b\sqrt{N}/20)^{-3/2}$. Solving this order unity relation (28) subject to the initial condition $\psi(\zeta, 0, \epsilon) = N_0 \operatorname{sech}^4 \zeta$ [$N_0 = N(\tau = 0)$] and boundary conditions $\psi(\pm\infty, \tau, \epsilon) = 0$, we obtain

$$\psi_0(\zeta, \tau_0, \tau_1) = N(\tau_1) \operatorname{sech}^4 \zeta. \quad (29)$$

This solution implies that ψ_0 does not depend on τ_0 , i.e., at the lowest order the solution is the same as (24).

Next the order ε relation yields

$$\frac{\partial \psi_1}{\partial \tau_1} + \mathcal{L}[\psi_1] = \mathcal{M}[\psi_0], \quad (30)$$

where $\psi_1(\pm\infty, \tau_0) = 0$, $\psi_1(\zeta, 0) = 0$, and

$$\begin{aligned} \mathcal{M}[\psi_0] = & -\left(\frac{\partial}{\partial \tau_1} + \frac{\zeta}{4N} \frac{\partial N}{\partial \tau_1} \frac{\partial}{\partial \zeta}\right) \psi_0 \\ & + \left(\frac{2}{\kappa}\right)^{1/3} \left(\int_{-\infty}^{\zeta} - \int_{-\infty}^{\infty}\right) \psi_0 d\zeta. \end{aligned} \quad (31)$$

Now for the existence of a solution of Eq. (30), its right-hand side must be perpendicular to the kernel of the operator $\mathcal{L}^\dagger[g] = 0$ [48] where \mathcal{L}^\dagger is the adjoint operator to \mathcal{L} given by

$$\mathcal{L}^\dagger \equiv \frac{1}{\kappa} \left(\frac{\partial^2}{\partial \zeta^2} + (30 \operatorname{sech}^2 \zeta - 16) \right) \frac{\partial}{\partial \zeta}. \quad (32)$$

The only solution of $\mathcal{L}^\dagger[g] = 0$, $g(\pm\infty) = 0$ is $g(\zeta) = \operatorname{sech}^4 \zeta$. From this orthogonality condition, we obtain

$$\int_{-\infty}^{+\infty} \operatorname{sech}^4 \zeta \mathcal{M}[\psi_0] d\zeta = 0. \quad (33)$$

This equation after integration and simplifications yields (with $\tau_1 = \varepsilon \tau$)

$$\frac{N(\tau)}{N_0} = \left(1 - \frac{\tau}{\tau_{\text{cr}}}\right)^4, \quad \tau_{\text{cr}} = \frac{9}{5\varepsilon} \sqrt{\frac{b\sqrt{N_0}}{5}}. \quad (34)$$

Here $N_0 = N(\tau = 0)$ is the initial amplitude. Thus the approximated solution of Eq. (21) is obtained as

$$\psi(\xi, \tau) = N(\tau) \operatorname{sech}^4 \left[\Delta(\tau)^{-1} \left(\xi - \frac{2b}{5} \int_0^\tau \sqrt{N} d\tau \right) \right]. \quad (35)$$

The amplitude $N(\tau)$ is given by Eq. (34), the width of the solitary pulse $\Delta(\tau)$ is given by

$$\Delta(\tau) = \Delta_0 \left(1 - \frac{\tau}{\tau_{\text{cr}}}\right)^{-1}, \quad \Delta_0 = \sqrt{\frac{20}{b\sqrt{N_0}}}, \quad (36)$$

and the energy [Eq. (23)] is given by

$$\mathcal{E}(\tau) = \mathcal{E}_0 \left(1 - \frac{\tau}{\tau_{\text{cr}}}\right)^7, \quad \mathcal{E}_0 = \frac{64N_0}{7\sqrt{5b}}, \quad (37)$$

where Δ_0 and \mathcal{E}_0 are the initial width and energy of the solitary pulse. It should be noted that for a solitary wave solution to exist one must have $\Delta > 0$ and $\mathcal{E} > 0$; therefore, the above solutions Eqs. (34), (36), and (37) are physically valid only for $\tau \lesssim \tau_{\text{cr}}$. Thus the approximated solution presented here clearly shows that the Lorentz force induced rotational effect causes the solitary wave amplitude (width), energy, and consequently velocity to decay (increase) algebraically with time $\tau \in [0, \tau_{\text{cr}})$ and at $\tau = \tau_{\text{cr}}$, the nonlinear wave collapses.

However, the value of τ_{cr} [Eq. (34)] provides a good estimation of a characteristic lifetime of an electrostatic ion cyclotron (EIC) solitary wave. In terms of the actual parameter, τ_{cr} can be written as

$$\tau_{\text{cr}} = \frac{7.2}{\Omega_i} \left(\frac{\rho_{si}}{\Delta_0} \right). \quad (38)$$

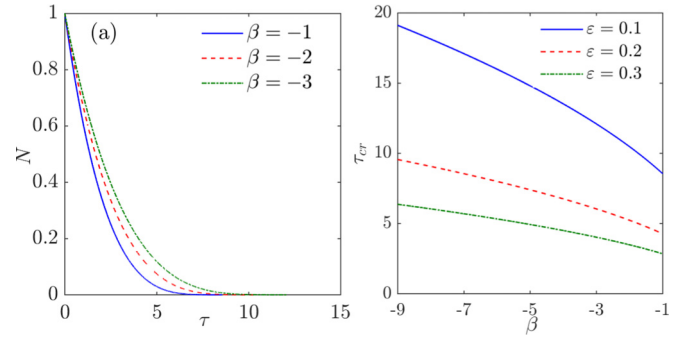


FIG. 1. (a) The time variations of amplitude for different values of β with $N_0 = 1$ and $\varepsilon = 0.1$. (b) Variation of critical time τ_{cr} with respect to β for different values of ε .

Thus the lifetime of an EIC solitary wave increases with the decrease (increase) of the strength of the magnetic field (trapping parameter b as $\Delta_0 \propto b^{-1/2}$). As an illustration the variations of N with time [$\tau \in (0, \tau_{\text{cr}})$] for different b are shown graphically in Fig. 1. The values of τ_{cr} for different values of ε and β are shown in Table I.

IV. NUMERICAL SOLUTIONS

In this section, we numerically simulate the SOE [Eq. (21)] with the help of a pseudospectral method in an interval $[-L, L]$. In this method, aliasing errors appear when dealing with a nonlinear term ($\psi^{3/2}$), where the wave number in the convolution exceeds the frequency range. Following the recipe of Ref. [49] dealiasing is used and an additional damping term

$$\gamma(\xi) = (\nu/2)[(1 + \tanh \mu \xi_-) + (1 - \tanh \mu \xi_+)] \quad (39)$$

is inserted on the left-hand side of Eq. (21) in the form $\partial_\xi \gamma$ to prevent the radiated wave effects in the computation [44]. Here $\xi_\pm = \xi \pm 7L/8$ and ν, μ are some constants. For computation, we take the number of grids (M) = 8192, spatial width = $2L/M$, temporal width = 10^{-4} , $\nu = 0.1$, $\mu = 24/L$, and $L = 800$ and observe bounded solutions.

First, we consider the initial pulse as

$$\psi(\xi, 0) = \operatorname{sech}^4(\sqrt{b/20} \xi). \quad (40)$$

The simulated results for different β (b) and ε are shown graphically in Figs. 2–5.

The simulated results at lower time $\tau = 0.1$ ($< \tau_{\text{cr}}$) for $\varepsilon = 0.1$ and 0.2 for different b are shown in Figs. 2 and 3, respectively. The solutions presented in both Figs. 2(a) and 2(b)

TABLE I. Values of τ_{cr} for different values of ε and β .

$B_0(10^{-5}T)$	ε	β	b	τ_{cr}
1.2	0.1	-1	1.13	8.48
1.2	0.1	-2	1.69	10.39
1.2	0.1	-3	2.25	12
2.2	0.3	-1	1.13	2.83
2.2	0.3	-2	1.69	3.46
2.2	0.3	-3	2.25	4

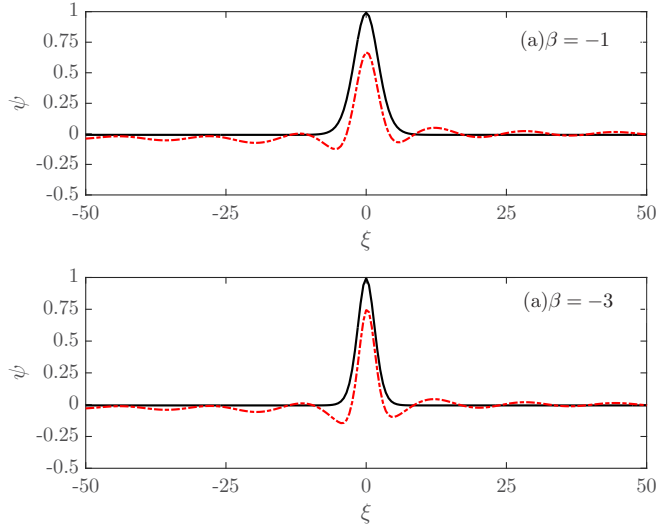


FIG. 2. Decaying of initial solitary pulse for $\varepsilon = 0.1$ and $\tau = 0.1$ ($< \tau_{cr}$).

and Figs. 2(c) and 2(d) clearly show the decrease (increase) in amplitude (width) of the solitary pulses. The comparison between the solutions in Figs. 2(a) and 2(b) [also in Figs. 3(a) and 3(b)] reveals that with the increase of the trapped particle represented through β (b), the decay rate is decreased. In a similar way, the comparative studies between the solutions in Figs. 2 and 3 show that with the increase of the strength of the magnetic field represented through ε , the decay rate is increased. All these results are in qualitative agreement with the analytical results which predict $\tau_{cr} \propto (\sqrt{b}, \varepsilon^{-1})$ [Eq. (34) and Table I].

The asymptotic analytical solutions predict that at $\tau \rightarrow \tau_{cr}$, the nonlinear wave collapses. Thus to observe the complete picture of the solutions at time close to τ_{cr} , we simulate Eq. (21) with $\beta = -1$ ($b = 1.13$) for different ε at larger times ($< \tau_{cr}$) and the solutions are shown in Figs. 4(a) and 4(b). These solutions clearly demonstrate the formation of oscil-

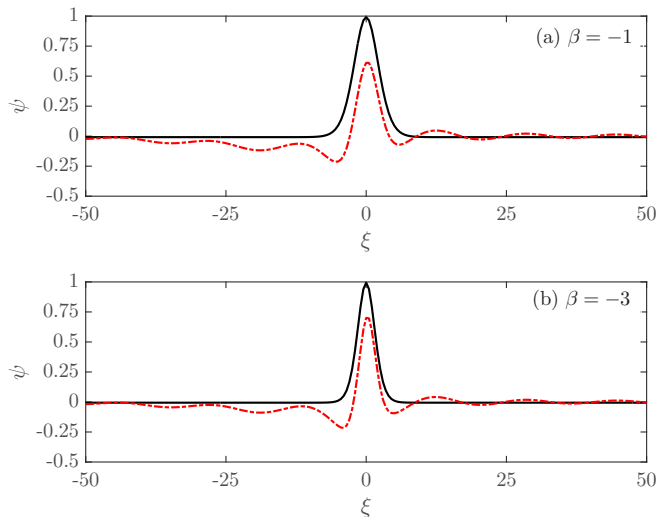


FIG. 3. Decaying of initial solitary pulse for $\varepsilon = 0.3$ and $\tau = 0.1$ ($< \tau_{cr}$).

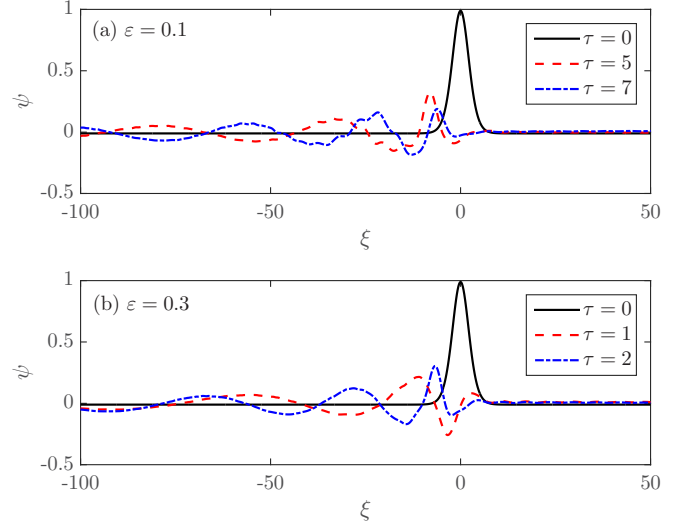


FIG. 4. Decaying of initial solitary pulse and generation of oscillatory trails for $\beta = -1$ in different time $\tau < \tau_{cr}$.

latory tails and this process is accelerated with the increase of the magnetic field.

It is to be noted that the approximated analytical results [Eq. (35)] do not provide any insight into the solutions beyond τ_{cr} (i.e., in the long time). To observe the long-time behavior, we simulate Eq. (21) for $\tau = 25$ and 50 . The solutions are shown graphically in Fig. 5. Interestingly, all the solutions reveal the formation of a multiharmonic and EICW packet in the downstream side as observed in Fig. 5 [curves in Figs. 5(a)–5(d)]. These solutions also show that with the increase of the number of trapped electrons (β), the nonlinear wave amplitude increases. The formation of wave packets in the large time is a clear indication of the EICW group dynamics.

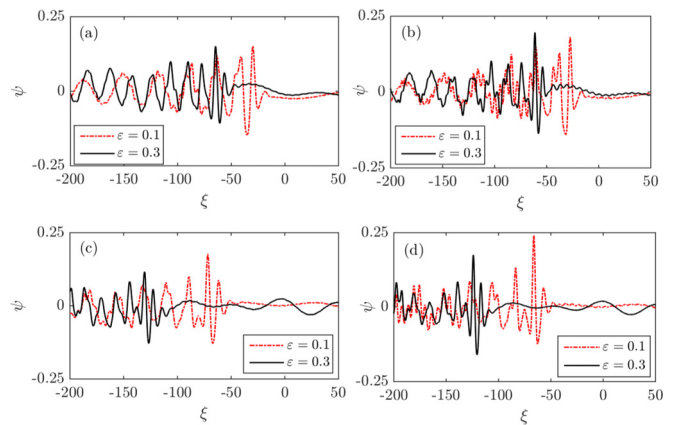


FIG. 5. Transition from initial solitary pulse to wave-packet formation after critical time ($\tau \gg \tau_{cr}$) for different values of ε . (a),(c) and (b),(d) correspond to $\beta = -1$ and $\beta = -2$, respectively. The upper and lower panels show the evolution of solitary pulse at $\tau = 25$ and $\tau = 50$, respectively.

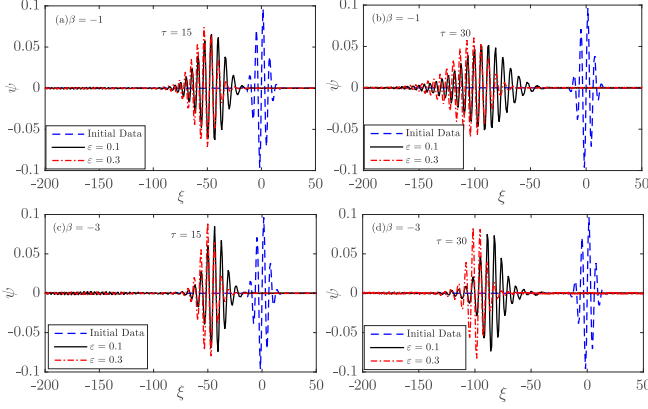


FIG. 6. Evolution of envelope initial profile in different time for different β and ε .

Finally to confirm the wave-packet dynamics, we simulate Eq. (21) with the initial profile

$$\psi(\xi, 0) = e^{-0.016\xi^2} \sin(1.005\xi). \quad (41)$$

The solutions are presented graphically in Fig. 6 which confirm the formation of wave packets in the long time. The solutions also reveal that the magnetic field increases the harmonics and trapped electrons increase the amplitude. The electric field $E(= -\partial_\xi \psi)$ structures corresponding to the potential ψ (Fig. 5) for different time, trapping parameter, and magnetic field are presented in Fig. 7. The E field profiles are qualitatively similar with those of the observed structures [12].

V. DISCUSSIONS

In this work, we have investigated the nonlinear transport dynamics of EICWs in the presence of Schamel distributed trapped electrons under the influence of weak magnetic field ($\Omega_i \ll \omega_{pi}$) in collisionless and homogeneous plasmas. The dynamics of the nonlinear wave is shown to be governed by a Schamel-Ostrovsky type equation [Eq. (21)], which is

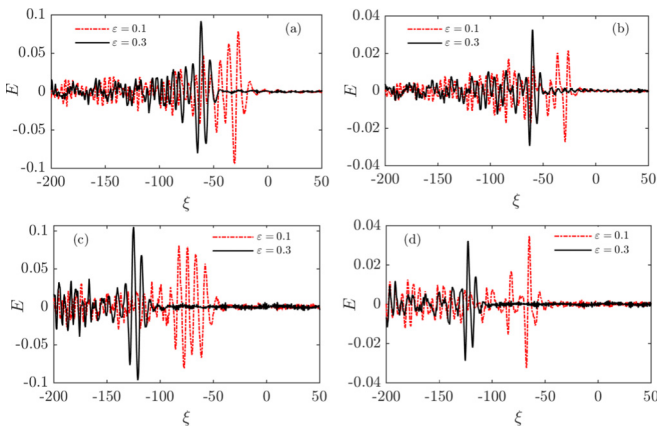


FIG. 7. The normalized electric field $E(= -\partial_\xi \psi)$ profile in different time for different ε and β . (a),(c) and (b),(d) correspond to $\beta = -1$ and $\beta = -2$, respectively. The upper and lower panels show the evolution of solitary pulse at $\tau = 25$ and $\tau = 50$, respectively.

a Lorentz force induced rotation modified Schamel equation [35]. This equation is not exactly integrable (solvable) as the energy of the nonlinear wave is not conserved [Eq. (23)] and thereby the equation is analyzed analytically using the KBM method [40]. The analytical solution predicts a critical time $\tau_{cr} \equiv \tau_{cr}(\Omega_i, b)$ [Eqs. (34) and (38)] below which the amplitude (width) of a localized (solitary) pulse decays (grows) with time (τ). The numerical solutions with the typical auroral plasma parameters confirm the analytical results (see Figs. 2 and 3).

The computational results are noteworthy, which predict the formation of oscillatory tails near τ_{cr} and then multi-harmonic waves and finally the wave packets (wave group dynamics) in the long time ($\tau \gg \tau_{cr}$) (see Figs. 4 and 5). This wave group dynamics (at time beyond the critical time) of nonlinear EICWs described through the derived SOE [Eq. (21)] is confirmed by the simulation with the modulated initial pulse [see Eq. (41) and Fig. 6].

The EICWs are observed in the auroral magnetosphere, characterized by the typical plasma parameters: $n_0 \sim 10^7 m^{-3}$, $T_{ef} \sim (10 \text{ eV} - 10 \text{ keV})$ and $B_0 \sim 10^{-5} T$ [6,10,11,20,21]. These values estimate $\lambda_D \sim 2.35 \sqrt{T_{ef}} m \sim (7.43 - 235)m$ and the electric field amplitude (in dimensional form) $\tilde{E} \sim 0.43 \sqrt{T_{ef}} E \text{ V m}^{-1}$ (E is the normalized electric field). The simulated results shown in Fig. 5 provide $E \sim 0.1$ for $\beta = -2$ ($b = 1.69$) and $\varepsilon = 0.3$ [Fig. 5(c)]. Thus $T_{ef} \sim 400 \text{ eV}$ estimates $\tilde{E} \sim 10^3 m \text{ V m}^{-1}$, which well agrees with the FAST satellite observations [10,13].

There have been many theoretical investigations [15–21] to study the observed spiky electric field structures associated to the EICWs in the absence of trapped electrons in auroral plasmas. An attempt has also been made to study the effect of trapped electrons on EICWs [39]. However, these approaches cannot explain how an EIC solitary wave collapses and generates multiharmonic as well as wave-packet structures. The present studies explain the mechanism of formation of multiharmonic and EICW packet structures and also estimate the lifetime of an EIC solitary wave. The analytical results reveal that the solitary wave energy completely vanishes at $\tau \sim \tau_{cr}$ [Eq. (37)]. Since the total energy is conserved [see Eq. (23)], in the large time ($\tau \gg \tau_{cr}$), the rate of change of Lorentz force induced rotational energy (\mathcal{E}_{rot}) increases. This increment in (\mathcal{E}_{rot}) generates the multiharmonics EICWs and finally, self-interactions among these harmonics form EIC wave packets. Thus the mechanism presented here could be an alternative physical mechanism for the spiky electric field structures of EICWs in auroral plasma. The wave collapse time (τ_{cr}) increases (decreases) with the increase of electron trapping (external magnetic field) (see Table I).

Finally, the low-frequency (0.1–5.0 Hz) electromagnetic ion cyclotron wave (EMICW) is also believed to be one of the dominant wave modes in the Earth's magnetosphere [50–52]. These waves are generated by (10–100 keV) ion distributions with temperature anisotropy [53]. The nonlinear behavior of these EMICWs is our future focus of investigation.

ACKNOWLEDGMENTS

The author (D.C.) would like to thank the Department of Science and Technology, Government of India for provid-

ing support from INSPIRE Fellowship (Ref. No. IF170300). The authors thank the referees for their careful reading

and for offering constructive suggestions to improve the manuscript.

-
- [1] F. F. Chen, *Introduction to Plasma Physics* (Plenum, New York, 1974).
- [2] N. D'Angelo and R. W. Motley, *Phys. Fluids* **5**, 633 (1962).
- [3] T. Ohnuma, S. Miyake, T. Sato, and T. Watari, *Phys. Rev. Lett.* **26**, 541 (1971).
- [4] M. Ono, *Phys. Rev. Lett.* **42**, 1267 (1979).
- [5] F. S. Mozer, C. W. Carlson, M. K. Hudson, R. B. Torbert, B. Parady, J. Yatteau, and M. C. Kelley, *Phys. Rev. Lett.* **38**, 292 (1977).
- [6] P. M. Kintner, M. C. Kelley, and F. S. Mozer, *Geophys. Res. Lett.* **5**, 139 (1978).
- [7] C. A. Cattell, F. S. Mozer, I. Roth, R. R. Anderson, R. C. Elphic, W. Lennartsson, and E. Ungstrup, *J. Geophys. Res.* **96**, 11421 (1991).
- [8] M. Andre, H. Koskinen, G. Gustafsson, and R. Lundin, *Geophys. Res. Lett.* **14**, 463 (1987).
- [9] F. S. Mozer, R. Ergun, M. Temerin, C. Cattell, J. Dombeck, and J. Wygant, *Phys. Rev. Lett.* **79**, 1281 (1997).
- [10] R. E. Ergun, C. W. Carlson, J. P. McFadden, F. S. Mozer, G. T. Delory, W. Peria, C. C. Chaston, M. Temerin, R. Elphic, R. Strangeway, R. Pfaff, C. A. Cattell, D. Klumpar, E. Shelley, W. Peterson, E. Moebius, and L. Kistler, *Geophys. Res. Lett.* **25**, 2025 (1998).
- [11] R. Pottelette and R. A. Treumann, *Geophys. Res. Lett.* **32**, L12104 (2005).
- [12] J. P. McFadden, C. W. Carlson, R. E. Ergun, C. C. Chaston, F. S. Mozer, M. Temerin, D. M. Klumper, E. G. Shelley, W. K. Peterson, E. Moebius, L. Kistler, R. Elphic, R. Strangeway, C. Cattell, and R. Pfaff, *Geophys. Res. Lett.* **25**, 2045 (1998).
- [13] C. W. Carlson, R. F. Pfaff, and J. G. Watzin, *Geophys. Res. Lett.* **25**, 2013 (1998).
- [14] M. C. Kelley, *The Earth's Ionosphere: Plasma Physics and Electrodynamics* (Academic, New York, 2009).
- [15] M. Temerin, M. Woldroff, and F. S. Mozer, *Phys. Rev. Lett.* **43**, 1941 (1979).
- [16] P. K. Chaturvedi, *Phys. Fluids* **19**, 1064 (1976).
- [17] M. Y. Yu, *J. Plasma Phys.* **18**, 139 (1977).
- [18] L. C. Lee and J. R. Kan, *Phys. Fluids* **24**, 430 (1981).
- [19] D. Jovanovic and P. K. Shukla, *Phys. Rev. Lett.* **84**, 4373 (2000).
- [20] R. V. Reddy, G. S. Lakhina, N. Singh, and R. Bharuthram, *Nonlin. Process. Geophys.* **9**, 25 (2002).
- [21] G. S. Lakhina, S. V. Singh, and A. P. Kakad, *Adv. Space Res.* **47**, 1558 (2011).
- [22] V. V. Gavrishchaka, G. I. Ganguli, W. A. Scales, S. P. Slinker, C. C. Chaston, J. P. McFadden, R. E. Ergun, and C. W. Carlson, *Phys. Rev. Lett.* **85**, 4285 (2000).
- [23] G. Ganguli, S. Slinker, V. Gavrishchaka, and W. Scales, *Phys. Plasmas* **9**, 2321 (2002).
- [24] H. Böhmer and S. Fornaca, *J. Geophys. Res.* **84**, 5234 (1979).
- [25] D. M. Suszcynsky, N. D'Angelo, and R. L. Merlino, *J. Geophys. Res.* **94**, 8966 (1989).
- [26] S. Kim, R. L. Merlino, and G. Ganguli, *Phys. Plasmas* **13**, 012901 (2006).
- [27] H. L. Rowland and P. J. Palmadesso, *J. Geophys. Res.* **92**, 299 (1987).
- [28] B. Eliasson and P. K. Shukla, *Phys. Rep.* **422**, 225 (2006).
- [29] H. Matsumoto, X. H. Deng, H. Kojima, and R. R. Anderson, *Geophys. Res. Lett.* **30**, 1326 (2003).
- [30] C. Cattell, J. Dombeck, J. Wygant, J. F. Drake, M. Swisdak, M. L. Goldstein, W. Keith, A. Fazakerley, M. André, E. Lucek, and A. Balogh, *J. Geophys. Res.* **110**, A01211 (2005).
- [31] J. F. Drake, M. Swisdak, C. Cattell, M. A. Shay, B. N. Rogers, and A. Zeiler, *Science* **299**, 873 (2003).
- [32] M. V. Goldman, D. L. Newman, and G. Lapenta, *Space Sci. Rev.* **199**, 651 (2016).
- [33] I. H. Hutchinson, *Phys. Plasmas* **24**, 055601 (2017).
- [34] F. S. Mozer, O. V. Agapitov, B. Giles, and I. Vasko, *Phys. Rev. Lett.* **121**, 135102 (2018).
- [35] H. Schamel, *Plasma Phys.* **14**, 905 (1972).
- [36] H. Schamel, *Phys. Rep.* **140**, 161 (1986).
- [37] H. Schamel, *J. Plasma Phys.* **9**, 377 (1973).
- [38] H. Schamel, *Phys. Scr.* **T2A**, 228 (1982).
- [39] S. Bujarbarua and M. Y. Yu, *Phys. Fluids* **25**, 884 (1982).
- [40] N. Bogoliubov, *Asymptotic Methods in the Theory of Non-Linear Oscillations* (Gordon and Breach, Paris, 1961).
- [41] L. Ostrovsky, *Oceanology* **18**, 119 (1978).
- [42] L. Ostrovsky and Y. A. Stepanyants, *Phys. D (Amsterdam, Neth.)* **333**, 266 (2016).
- [43] M. A. Obregon and Y. A. Stepanyants, *Phys. Lett. A* **249**, 315 (1998).
- [44] R. Grimshaw, Y. Stepanyants, and A. Alias, *Proc. R. Soc. A* **472**, 20150416 (2015).
- [45] A. I. Zemlyanukhin, A. V. Bochkarev, I. V. Andrianov, and V. I. Erofeev, *J. Sound Vib.* **491**, 115752 (2021).
- [46] E. Ott and R. N. Sudan, *Phys. Fluids* **12**, 2388 (1969).
- [47] D. E. Pelinovsky and R. Grimshaw, *Phys. D (Amsterdam, Neth.)* **98**, 139 (1996).
- [48] E. L. Ince, *Ordinary Differential Equations* (Dover, New York, 1956).
- [49] J. P. Boyd, *Chebyshev and Fourier Spectral Methods* (Dover, New York, 2001).
- [50] B. Grison, O. Santolík, J. Lukačević, and M. E. Usanova, *Geophys. Res. Lett.* **48**, e2020GL090921 (2021).
- [51] M. E. Usanova, I. R. Mann, J. Bortnik, L. Shao, and V. Angelopoulos, *J. Geophys. Res.* **117**, A10218 (2012).
- [52] R. E. Erlandson and A. J. Ukhorskiy, *J. Geophys. Res.* **106**, 3883 (2001).
- [53] J. M. Cornwall, *J. Geophys. Res.* **70**, 61 (1965).